Supplementary Materials: fMRI responses during perceptual decision-making at 3 and 7 Tesla in human cortex, striatum, and brainstem

Authors: Olympia Colizoli[a,b,c], Jan Willem de Gee[a,b], Wietske van der Zwaag[d], Tobias H. Donner[a,b,e]*

Affiliations:

[a] Section Computational Cognitive Neuroscience, Department of Neurophysiology and Pathophysiology, University Medical Center Hamburg-Eppendorf, Hamburg, Germany

[b] Department of Psychology, University of Amsterdam, Amsterdam, The Netherlands

[c] Donders Institute for Brain, Cognition and Behaviour, Radboud University Nijmegen, The Netherlands

[d] Spinoza Centre for Neuroimaging, Amsterdam, The Netherlands

[e] Amsterdam Brain & Cognition, University of Amsterdam, Amsterdam, The Netherlands

Corresponding Authors:

*Olympia Colizoli
Radboud University Nijmegen
Donders Centre for Cognition
Thomas van Aquinostraat 4
6525 GD Nijmegen
olympia.colizoli@donders.ru.nl

*Tobias H. Donner
University Medical Center Hamburg-Eppendorf
Department of Neurophysiology and Pathophysiology, N43
Martinistraße 52
20246 Hamburg
t.donner@uke.de

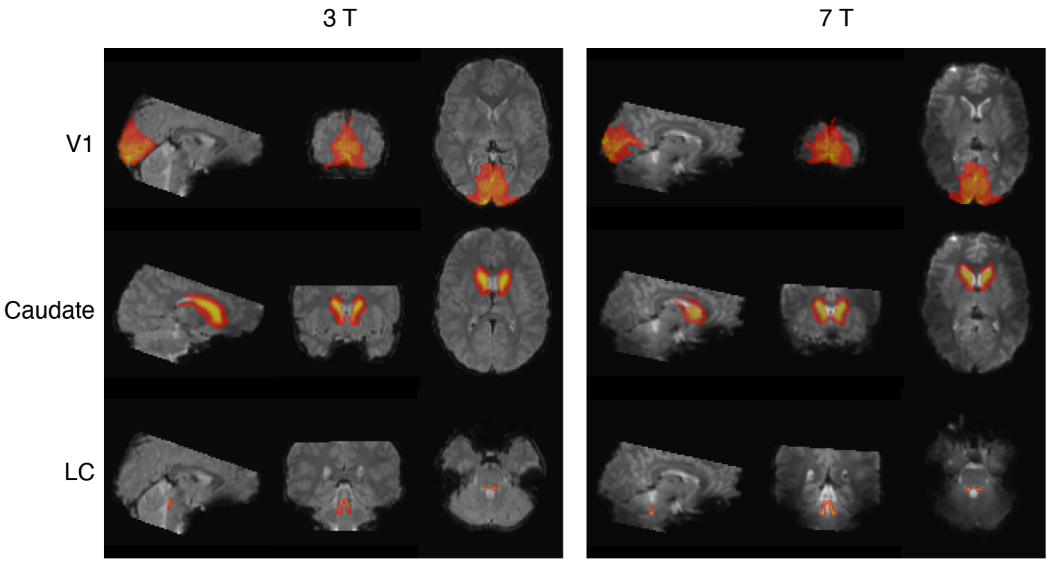

Supplementary Fig. 1. Example of affine registration to T1-weighted MNI-152 2-mm space. One participant's data is shown for one session of the 3 T and 7 T acquisitions on the left and right, respectively. One probabilistic ROI mask is show for each one of our ROI groups of interest: V1 for the cortical regions, caudate for the striatum, and the locus coeruleus (LC) for the brainstem nuclei.

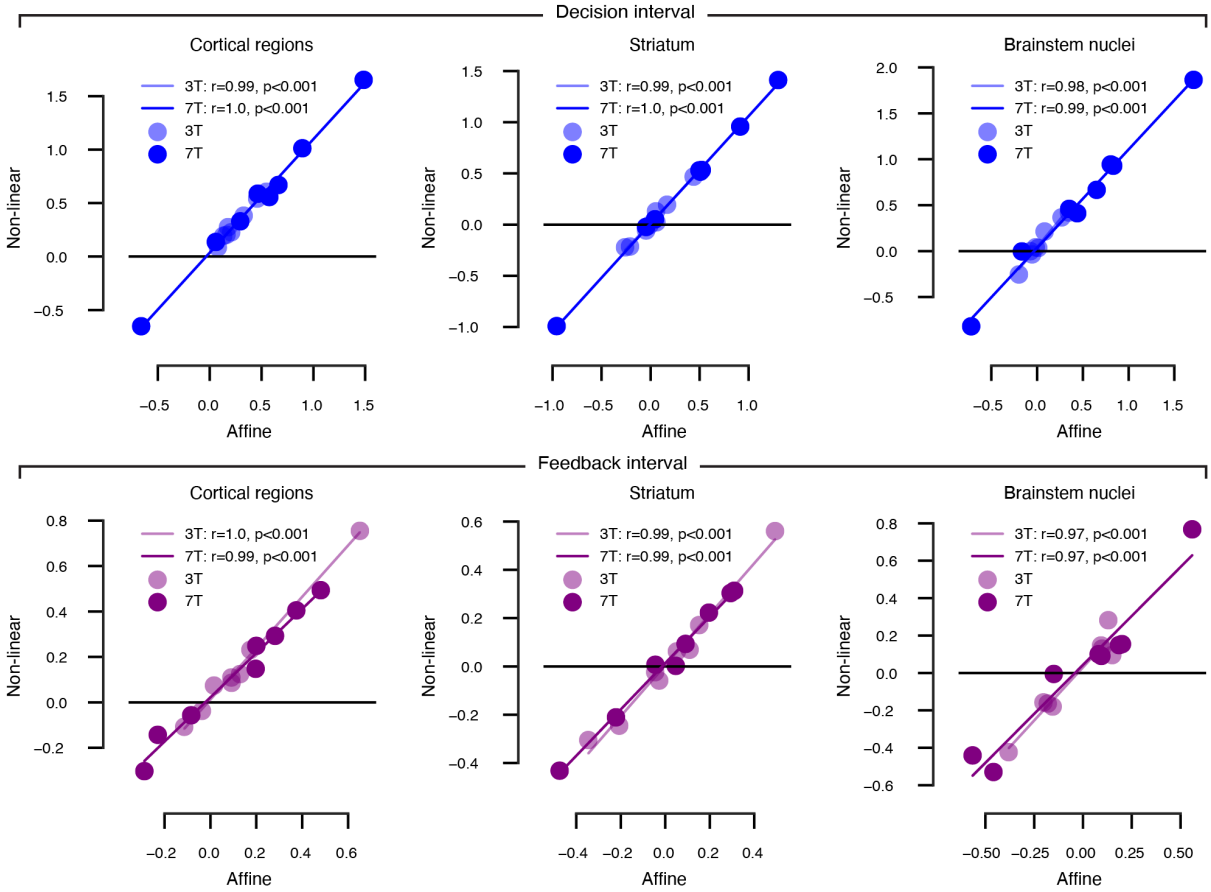

Supplementary Fig. 2. Affine as compared with non-linear registration to T1-weighted MNI-152 2-mm space. We assessed the effect of our choice of registration algorithm on the task-evoked responses in the ROI groups at each field strength (with regards to the data shown in Fig. 3). Individual dots are participants. The lines are the linear fits across participants for each contrast of interest (top row: stimulus vs. implicit baseline, bottom row: feedback vs. implicit baseline) within the corresponding ROI group at each field strength.

Characterizing temporal signal-to-noise ratio (tSNR)

TSNR is commonly used as a proxy for fMRI image quality (Triantafyllou et al., 2005; Vu et al., 2017) and has frequently been compared between field strengths (Brooks et al., 2013). By dividing the temporal mean of the fMRI signal by its temporal variability across a run, this measure quantifies the stability of the signal (albeit being affected by different noise sources). We also compared tSNR between the 3 T and 7 T acquisitions in an additional analysis. To this end, we used the residual signal fluctuations remaining after fitting the GLM used for quantifying the evoked responses described in the previous section (see Methods for details). We analyzed tSNR across the brain at the single-voxel level and at the level of the ROIs for which we evaluated the evoked responses.

The same preprocessing steps described in the main methods (see Methods section 2.6) applied to the data for the tSNR analysis with the following exceptions: Task effects in the data were removed by including two additional nuisance regressors: the task-evoked responses locked to the stimulus and feedback onsets convolved with a double gamma hemodynamic response function (HRF; 32 s kernel, peak amplitude of 1 at 6 s, undershoot amplitude 1/6th of response size at 16 s). The amplitude of the stimulus-locked response was modulated by reaction times (RT) on a trial-by-trial basis.

We computed tSNR as the mean of the time series divided by its standard deviation of residual, ongoing fMRI signal fluctuations, after accounting for the evoked responses as described above. The number of volumes (TRs) included in the computation was equalized across data sets for each participant (according to the minimum number of volumes of either the 3 T-A, 3 T-B or 7 T acquisitions within each session). For each participant and data set, the tSNR of each voxel was computed from the preprocessed time series for each session and then averaged across sessions. This resulted in one tSNR volume per participant per data set.

For the whole-brain analysis, the mean tSNR of the 3 T-A and 3 T-B data sets were subsequently averaged (voxel-wise) in order to compare the 7 T data set to a single 3 T data set. At the whole-brain level, the difference in tSNR for the mean 3 T data set was formally compared with the 7 T data set by means of a non-parametric one-sample permutation test with 5000 permutations and variance smoothing (5 mm), separately for the positive and negative directions (Randomise, FSL). The FWE rate (p-value threshold = .05) was controlled using the threshold-free cluster enhancement method (TFCE, FSL). Variance smoothing was applied to the resulting t-maps for the whole-brain analysis of tSNR, as per recommendation by FSL for small samples (< 20).

For the ROI-level analysis, the mean tSNR value within each ROI (see Methods section 2.8) was weighted based on the probability values of the individual voxels. Subsequently, the tSNR values of the 3 T-A and 3 T-B data sets were averaged in order to compare the 7 T data set to a single 3 T data set. Differences in tSNR were evaluated in a two-way repeated measures ANOVA with factors ROI group (levels: cortical regions, striatum, and brainstem nuclei) and field strength (levels: 3 T vs. 7 T). Planned comparisons for ROIs were done by means of a non-parametric two-tailed permutation test (10,000 permutations, custom Python code). No spatial smoothing was applied for the ROI analyses.

Comparison of tSNR at 3 T and 7 T for different brain regions

No significant difference in tSNR between field strengths was present in any region at the whole-brain level (Supplementary Fig. 3). Please note that the 7 T voxels were 1.8-fold smaller as compared with the 3 T acquisition, still leading to about the same tSNR.

At the level of ROIs, we found a significant interaction between ROI group and field strength (Supplementary Fig. 4A). A main effect of ROI group was observed. The main effect of field strength was not significantly significant. TSNR was higher for the 7 T acquisition as compared with 3 T within the brainstem ROI group, while the tSNR for the 3 T acquisition was higher as compared with 7 T within the cortical regions and striatum (Supplementary Fig. 4B-D for the individual ROIs).

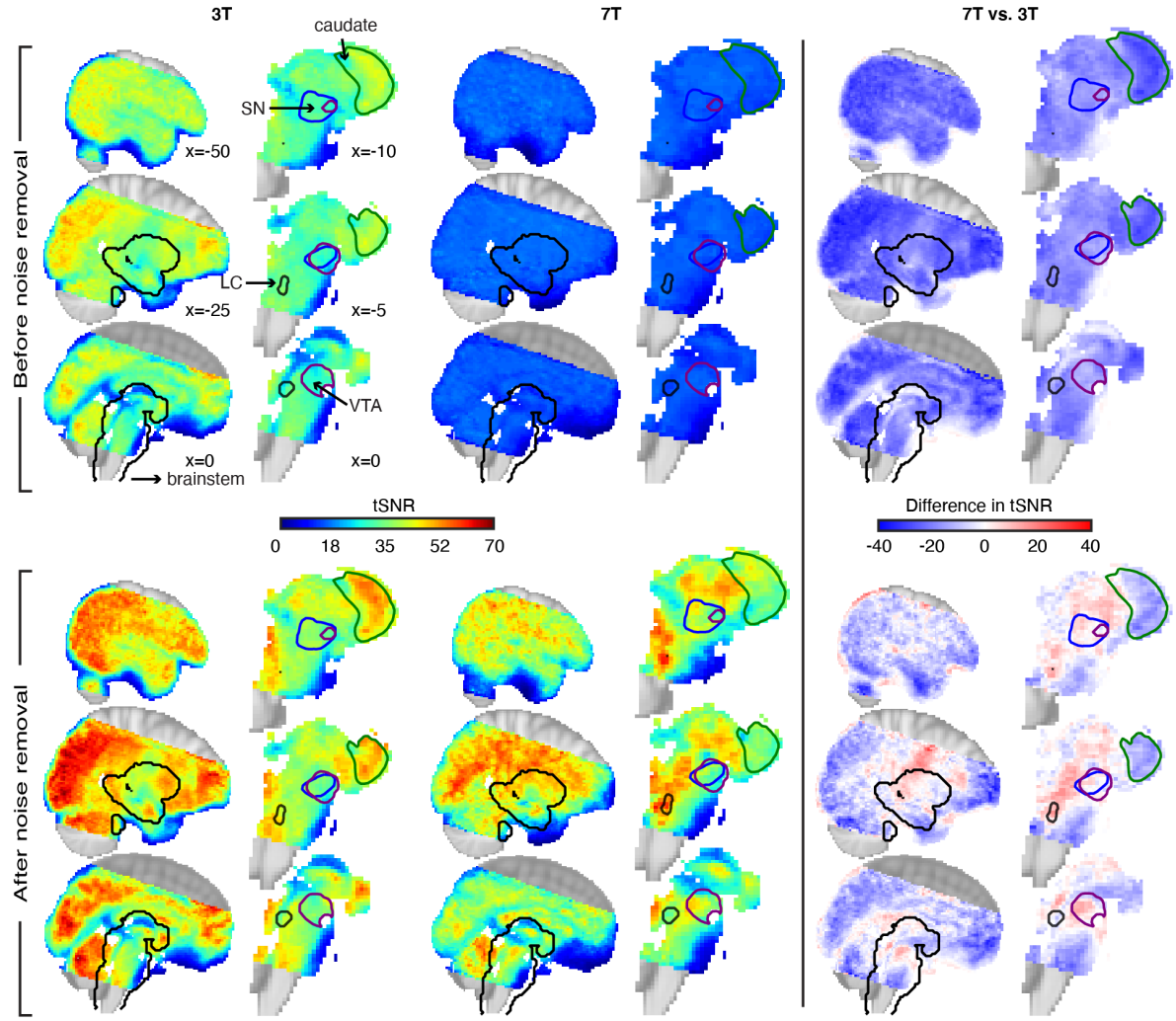

Supplementary Fig. 3. Spatial distribution of the temporal signal-to-noise ratio (tSNR) during the 2AFC task before and after noise removal. (Top row) tSNR distributions for the 3 T and 7 T data sets at the whole-brain level before noise removal (N = 8). (Bottom row) tSNR distributions after noise removal. The subcortical partition (black outlines) is extracted and magnified for the brainstem structures. Structures are labeled based on probabilistic atlases, including the caudate, locus coeruleus (LC), substantia nigra (SN), and ventral tegmental area (VTA). Colored regions indicate the common field of view of the 3 T and 7 T acquisitions (MNI152 brain as background).

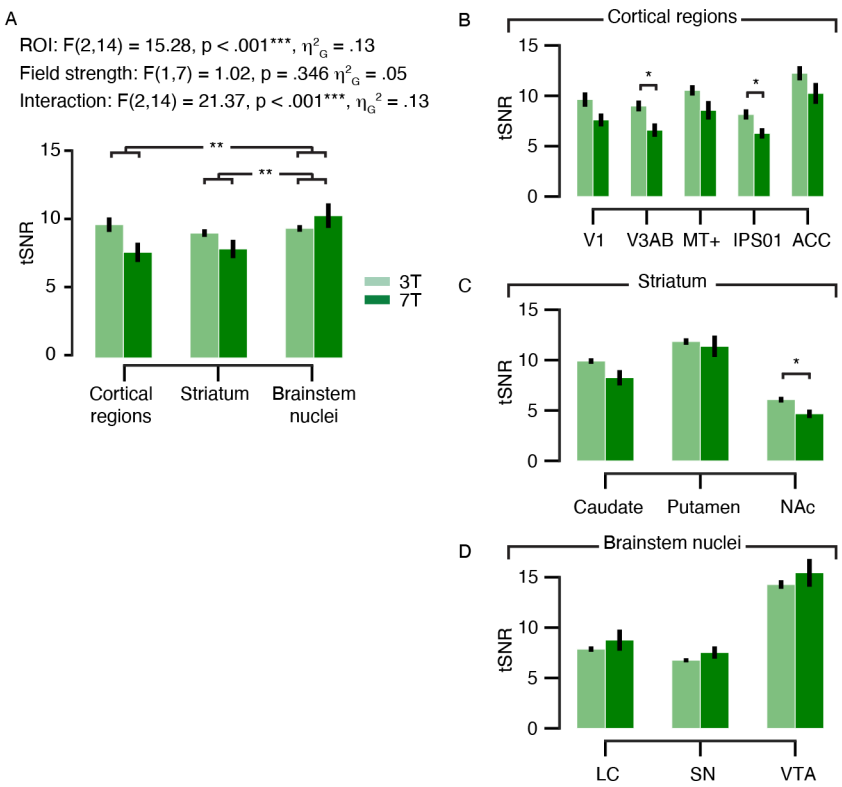

Supplementary Fig. 4. Temporal signal-to-noise ratio (tSNR) for 3 T and 7 T acquisition during the motion discrimination task. (**A**) tSNR per ROI group (cortical regions, striatum, and brainstem nuclei) and field strength after noise removal. Two-way repeated measures ANOVA results: F-statistics, main effect of ROI group, fMRI field strength, and their interaction. (**B**) Cortical regions (**C**) Striatum. NAc, nucleus accumbens. (**D**) Brainstem nuclei. LC, locus coeruleus. SN, substantia nigra. VTA, ventral tegmental area. Planned comparisons: *$p < .05$, **$p < .01$ (two-tailed permutation tests). Error bars, s.e.m. ($N = 8$).

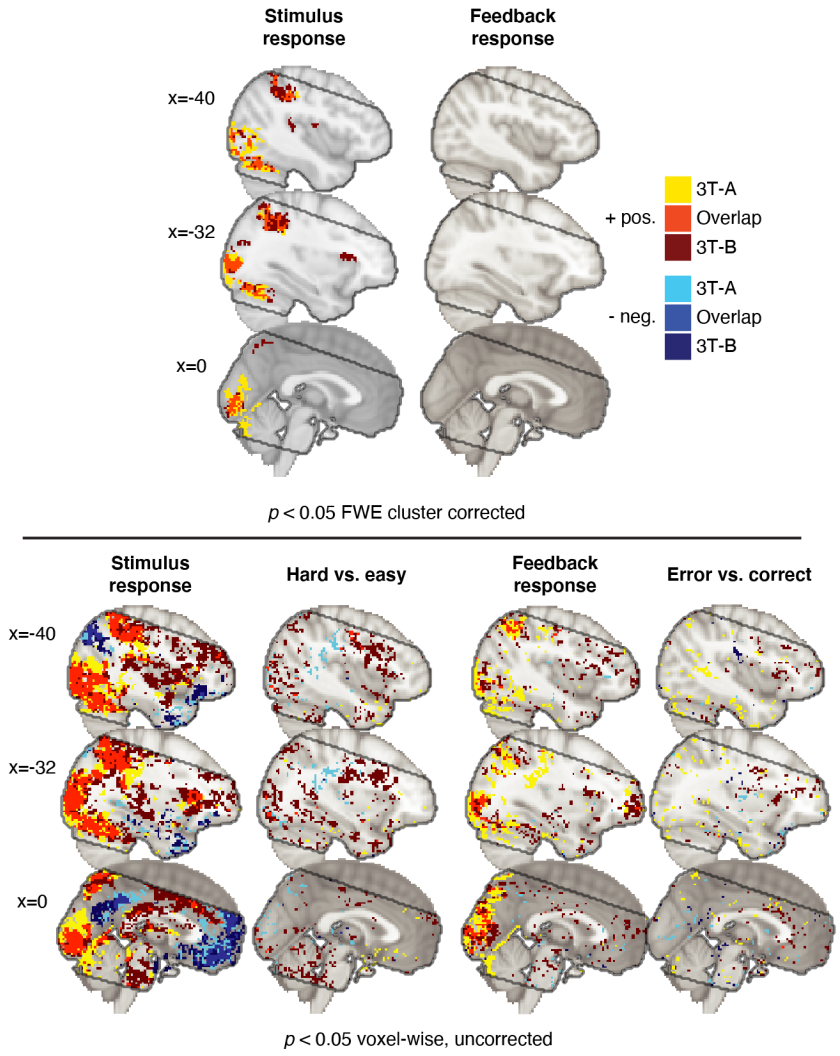

Supplementary Fig. 5. **Whole brain results of the task-evoked responses for the 3 T acquisition.** Contrasts of interest were investigated in a GLM analysis with an equal number of trials for each data set per participant (*N* = 8). (Top) Voxels surviving cluster-correction are shown for the 3 T-A and 3 T-B data sets for the stimulus and feedback responses, from the decision and post-feedback interval, respectively ($p < .05$, FWE, corrected). (Bottom) Voxels significant before cluster-correction for all contrasts of interest ($p < .05$, voxel-wise, uncorrected). The grey outline indicates the common field of view of the 3 T and 7 T acquisitions (MNI152 brain as background).

Supplementary Table 1. Conditions of the task-evoked responses during perceptual decision-making. Mean parameter estimates (standard deviation in parentheses) are given for each region of interest (ROI) and field strength ($N = 8$). The probability-weighted volume (mm^3) is indicated per ROI (MNI152 2-mm space). See Methods section 2.8 for details on ROIs.

ROI	Prob.-weighted volume	Field strength	Easy	Hard	Correct	Error
V1	11097.33	3 T	24.54 (15.17)	20.43 (11.29)	37.47 (27.43)	26.18 (33.11)
		7 T	50.42 (46.33)	34.52 (51.38)	41.95 (47.15)	16.31 (67.20)
V3AB	7175.8	3 T	16.19 (12.64)	13.81 (4.96)	19.35 (27.08)	17.01 (38.23)
		7 T	34.70 (43.51)	22.02 (48.60)	19.79 (29.37)	2.25 (67.77)
MT+	5949.33	3 T	21.59 (16.68)	18.32 (12.44)	9.95 (20.62)	10.27 (35.36)
		7 T	45.65 (45.93)	30.34 (47.99)	15.31 (33.81)	-4.83 (86.83)
IPS01	8888.91	3 T	13.92 (12.13)	12.88 (6.68)	11.91 (24.00)	12.76 (28.33)
		7 T	42.11 (49.16)	22.76 (48.32)	12.11 (28.76)	0.04 (73.14)
ACC	16603.38	3 T	3.89 (13.46)	2.84 (14.39)	-6.06 (36.81)	8.52 (48.50)
		7 T	93.69 (84.45)	52.97 (85.05)	28.43 (35.15)	-4.92 (156.36)
Caudate	8391.88	3 T	4.06 (18.28)	5.22 (17.31)	5.86 (39.22)	6.50 (31.28)
		7 T	57.38 (67.93)	31.42 (69.25)	6.89 (31.54)	-10.22 (105.65)
Putamen	13211.52	3 T	-1.32 (16.86)	1.17 (10.80)	5.99 (36.30)	5.60 (33.12)
		7 T	52.32 (64.42)	26.23 (69.01)	16.18 (27.21)	-27.26 (103.13)
NAc	1643.52	3 T	3.51 (11.08)	3.47 (9.11)	2.37 (23.87)	0.84 (18.93)
		7 T	32.32 (37.75)	17.58 (43.51)	5.34 (10.89)	-15.63 (56.19)
LC	224.26	3 T	2.65 (12.80)	8.39 (6.83)	5.47 (12.86)	5.78 (45.89)
		7 T	50.16 (73.27)	27.78 (71.86)	1.80 (63.60)	-26.39 (68.19)
SN	1772.9	3 T	3.35 (15.54)	1.16 (15.27)	-13.07 (37.76)	-2.98 (42.27)
		7 T	50.40 (46.15)	21.94 (44.65)	12.03 (31.17)	-27.27 (82.55)
VTA	2232.96	3 T	3.27 (24.81)	4.83 (30.05)	-28.52 (81.33)	-15.71 (95.34)
		7 T	132.14 (134.78)	42.47 (113.47)	11.91 (99.78)	-70.01 (187.70)
Cortical regions		3 T	16.03 (12.87)	13.66 (7.70)	14.53 (25.24)	14.95 (32.02)
		7 T	53.32 (52.14)	32.52 (54.99)	23.52 (28.83)	1.77 (85.74)
Striatum		3 T	2.08 (14.71)	3.29 (11.38)	4.74 (32.22)	4.31 (26.03)
		7 T	47.34 (56.14)	25.08 (60.23)	9.47 (20.18)	-17.70 (86.75)
Brainstem nuclei		3 T	3.09 (12.33)	4.80 (15.06)	-12.04 (42.84)	-4.30 (46.50)
		7 T	77.57 (83.80)	30.73 (76.16)	8.58 (61.42)	-41.22 (106.45)

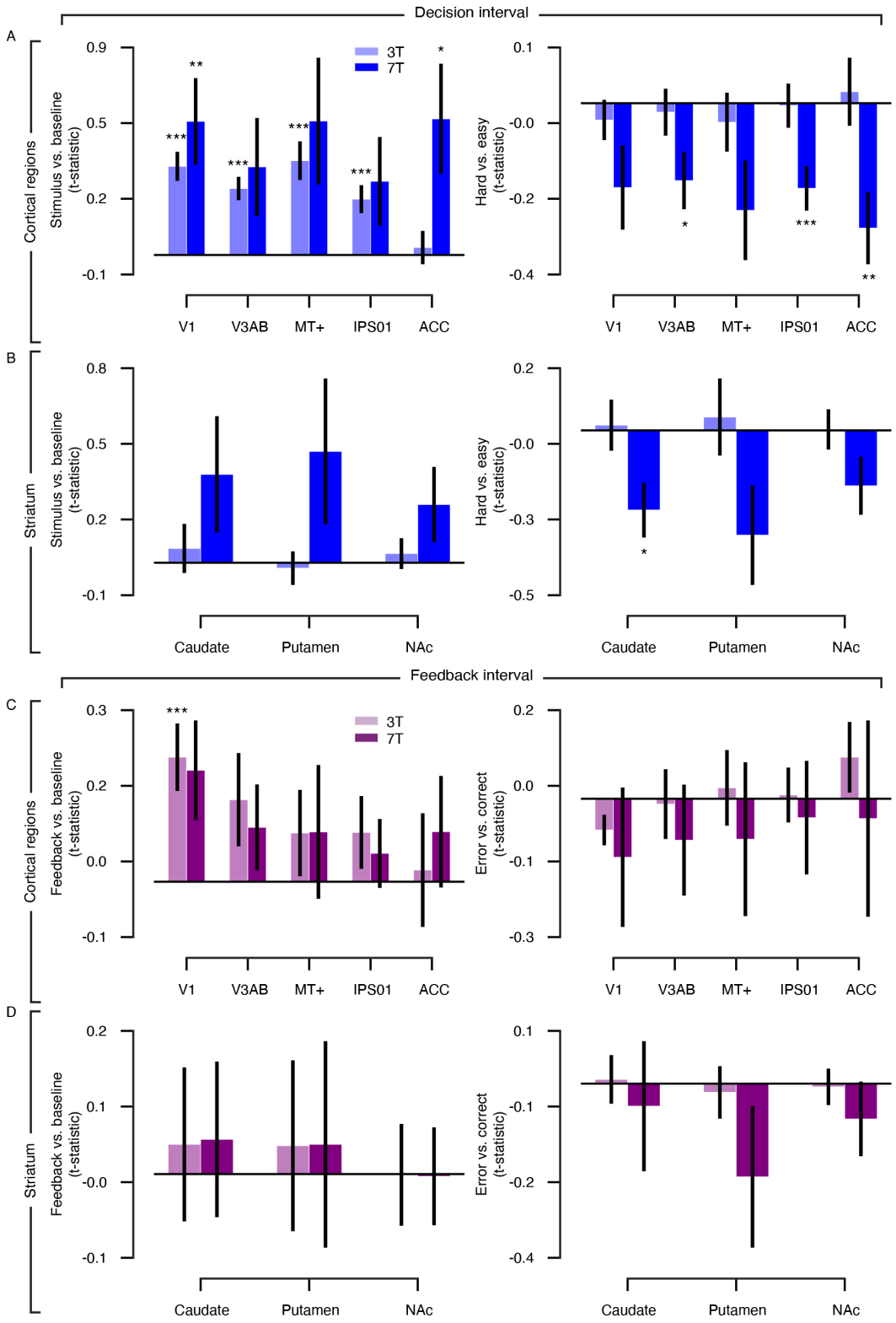

Supplementary Fig. 6. Task-evoked responses for 3 T and 7 T acquisition in cortical regions and striatum. (**A, B**) For the decision interval (stimulus-locked), the overall response and amplitude differences between hard vs. easy trials were investigated in cortical regions (A) and the striatum (B). NAc, nucleus accumbens. (**C, D**) For the post-feedback interval, the overall response and amplitude differences between error vs. correct trials were investigated in cortical regions (C) and the striatum (D). No field-strength differences were obtained (two-tailed permutation tests). The 3 T data are the mean of the 3 T-A and 3 T-B data subsets. Error bars, s.e.m. ($N = 8$).

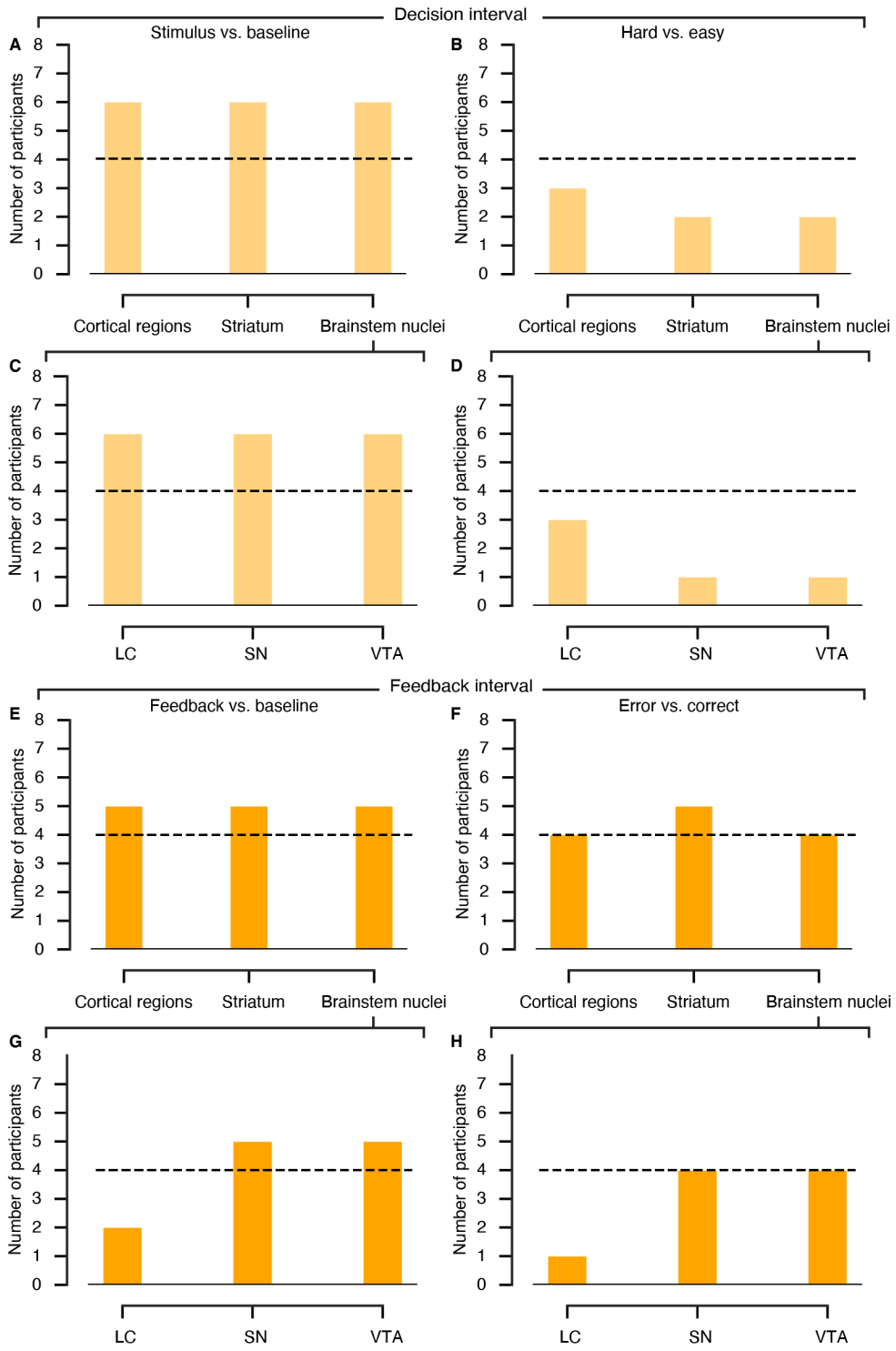

Supplementary Fig. 7. Number of participants who had greater or equal 7 T as compared with 3 T task-evoked responses during perceptual decision-making. The number of participants ($N = 8$) showing greater or equal task-evoked responses (t-statistic; see Fig. 3 and Fig. 4) for the 7 T as compared with the 3 T acquisition within each ROI group and brainstem nuclei for each contrast of interest in the decision interval (**A-D**) and the feedback interval (**E-G**). The dashed line represents the cutoff for an equal number of participants. Note that the differential responses (hard vs. easy, error vs. correct) were overall negative in direction for the 7 T acquisition in Fig. 3 and Fig.4.

References

Brooks, J., Faull, O., Pattinson, K., Jenkinson, M., 2013. Physiological Noise in Brainstem fMRI. Front. Hum. Neurosci. 7, 623. https://doi.org/10.3389/fnhum.2013.00623

Triantafyllou, C., Hoge, R.D., Krueger, G., Wiggins, C.J., Potthast, A., Wiggins, G.C., Wald, L.L., 2005. Comparison of physiological noise at 1.5 T, 3 T and 7 T and optimization of fMRI acquisition parameters. NeuroImage 26, 243–250. https://doi.org/10.1016/j.neuroimage.2005.01.007

Vu, A.T., Jamison, K., Glasser, M.F., Smith, S.M., Coalson, T., Moeller, S., Auerbach, E.J., Uğurbil, K., Yacoub, E., 2017. Tradeoffs in pushing the spatial resolution of fMRI for the 7T Human Connectome Project. Clean. FMRI Time Ser. Mitigating Noise Adv. Acquis. Correct. Strateg. 154, 23–32. https://doi.org/10.1016/j.neuroimage.2016.11.049